Macromolecular Nanocapsule Derived from Hyperbranched Polyethylenimine (HPEI): Mechanism of Guest Encapsulation versus Molecular Parameters

Decheng Wan,* Junjie Yuan, and Hongting Pu

Institute of Functional Polymers, School of Materials Science and Engineering, Tongji University, 1239 Siping Road, Shanghai 200092, China

Received October 6, 2008; Revised Manuscript Received January 15, 2009

ABSTRACT: Nanocapsule derived from hyperbranched polymer bears a number of active functional groups in the core; such a structure feature renders it possible to meticulously engineer the core of the nanocapsule and thus provides a unique opportunity to evaluate the structure−property relationship. Here the amino protons of HPEI (M_n = 10 000 Da) are 15%, 30%, 60%, and 86% alkylated with 2-dodecyloxymethyloxirane, leading to core−shell structured amphiphilic macromolecules (CAMs) with such different shell density as HP(EI-$OH_{0.15}C12_{0.15}$) (**3a**), HP(EI-$OH_{0.30}C12_{0.30}$) (**3b**), HP(EI-$OH_{0.60}C12_{0.60}$) (**3c**), and HP(EI-$OH_{0.86}C12_{0.86}$) (**3d**), respectively. The cores of **3a**−**3d** are further chemically modified by complete alkylation of the residual amino protons with propylene oxide, leading to HP(EI-$OH_1C12_{0.15}$) (**4a**), HP(EI-$OH_1C12_{0.30}$) (**4b**), HP(EI-$OH_1C12_{0.60}$) (**4c**), and HP(EI-$OH_1C12_{0.86}$) (**4d**), respectively. Nanocapsule with thick shell is also obtained by alkylation of HPEI with epoxy polystyrene (M_n = 1800), leading to HPEI with 15% (HP(EI-$OH_{0.15}PS_{0.15}$), **7a**), 30% (HP(EI-$OH_{0.30}PS_{0.30}$), **7b**), and 60% (HP(EI-$OH_{0.60}PS_{0.60}$), **7c**) of the amino protons being alkylated. Water-soluble, anionic dyes can be encapsulated by these CAMs. It is found that **7a**−**7c** exist as unimolecular inverted micelles in the tested range while **3a**−**3d** and **4a**−**4d** exist as aggregates in chloroform, indicating that a thick shell is crucial to the nature of unimolecular micelle. It is also found that the guest releasing ability is dependent on the nature of the functional groups in the core but independent of the shell density; thus, encapsulation of methyl orange by **3a**−**3c** is reversible, while that by **4a**−**4c** is irreversible. Congo red can be encapsulated by the aggregate of **3a**−**3d** or **4a**−**4d**, but excessive Congo reds cause precipitation of the aggregate. Finally, it is noticed that the molecule recognition property is also dependent on the nature of the functional groups in the core but independent of the shell density and shell thickness; as a result, a CAM with a designed core can highly selectively encapsulate a guest from a mixture.

Introduction

Core−shell structured amphiphilic macromolecule (CAM) derived from dendrimer or hyperbranched polymer has evoked much interest in supramolecular host−guest chemistry recently.[1] CAM is unique as a supramolecular host because (1) unlike a linear counterpart, CAM can accommodate a guest via noncovalent interaction partly due to its topological feature[2] and (2) unlike a physical micelle, CAM hardly collapses in rigorous environment due to the nature of covalent bond.

The guest encapsulation by dendrimer or dendrimer-based CAM has been intensively studied.[3] Meijer et al.[3c,d] synthesized a "dendritic box" by functionalization the terminal groups of polypropylenimine (PPI) dendrimer, and the resulting dendritic box could release the locked-in guests only via a size selective manner arising from shell congestion. Aida et al.[3e] also proved, by fluorescence quenching experiment, that the morphology of dendrimer framework evolved from "open" to "semiclosed" to "closed" with the increase of dendrimer generation. Generally speaking, the shell density of a dendrimer is important in guest selection, which can render the core an isolated microenvironment accessible only to special guests.

Hyperbranched polymer,[4] known for its multifunctionality, special topology, cost-effective production, and wide availability, can be a substitute of dendrimer and is now among the most popular parent compounds for the construction of CAM.[5] Such CAM has been widely used as a host for entrapping of various guests, but the mechanism[5d,6] seems to be rather different from that of dendritic box. Three issues need clarifying for CAMs derived from hyperbranched polymer: (1) whether the guest selection of CAM is due to the degree of functionalization (DF, or in other words, shell density), the nature of the functional groups (FGs) in the core, or both; (2) what is the underlying factor that determines the reversibility of the encapsulation, the DF, the FG, or the synergic effect of both DF and FG; (3) what factor directs a CAM to aggregate or to unimolecular (inverted) micelle.[1f,5a] To elucidate the above-mentioned three issues, we here synthesize a variety of CAMs by chemical derivation of a HPEI; the molecular parameters of the CAMs are chemically adjusted in terms of shell thickness, shell density (DF), and nature of the FGs in the core. The role of shell thickness and

Chart 1

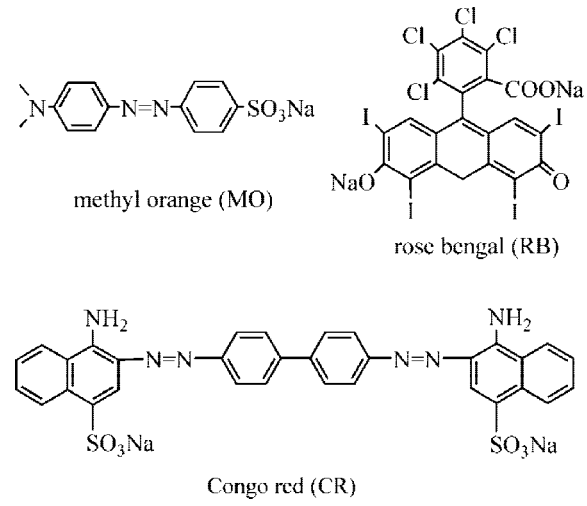

* Corresponding author: e-mail wandecheng@ tongji.edu.cn, Fax ++86 21 65982461.

10.1021/ma8026707 CCC: $40.75
Published on Web 02/16/2009

Scheme 1. Synthesis of CAMs

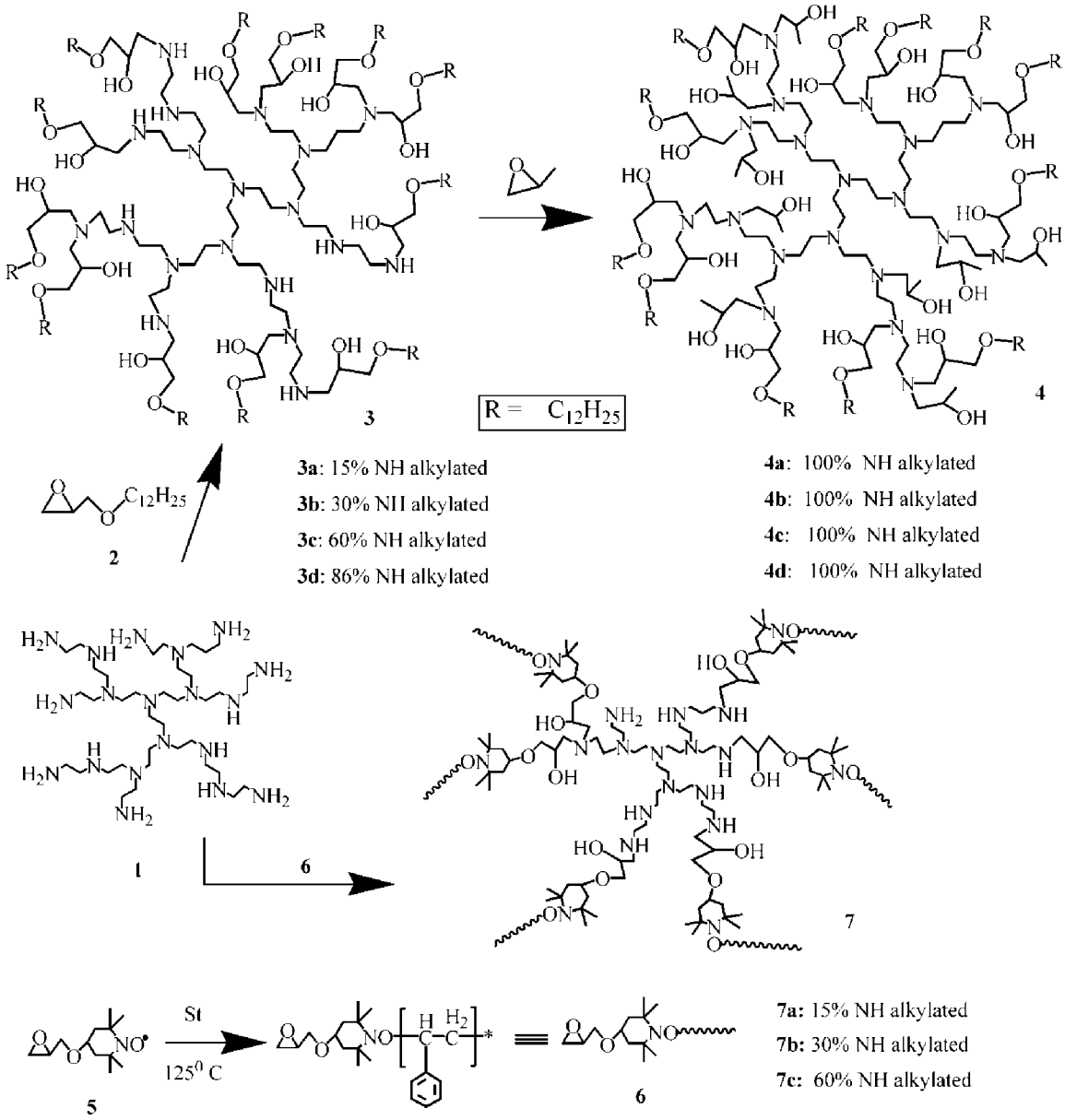

shell density has been described in a number of literatures,[5a−d,g] but the role of FGs in the core has rarely been discussed.[5i] Unlike dendrimer, micelle, or other core−shell structured polymer, hyperbranched polymer is structurally featured by having active FGs distributed core through shell. Specially, the FGs in the core can serve as a unique platform to achieve core-engineered CAMs, rendering intensive evaluation of the structure−property relationship possible, for example, for learning how an encapsulation switches from reversible to irreversible, how the solution behavior is directed from aggregate to unimolecularity, and how guest selection is realized.

Results and Discussion

1. Synthesis of CAMs. It was noticed previously[5i] that the reaction of HPEI (**1**) with an epoxy compound of **2** (Scheme 1) conveniently led to HP(EI-$OH_{0.15}C12_{0.15}$)[7] (**3a**), HP(EI-$OH_{0.30}$-$C12_{0.30}$) (**3b**), HP(EI-$OH_{0.60}C12_{0.60}$) (**3c**), and HP(EI-$OH_{0.86}$-$C12_{0.86}$) (**3d**). It was also found that **3d**, with a DF up to 86%, could highly selectively separate anionic, water-soluble dyes such as CR, MO, and RB (Chart 1) from a mixture of cationic methylene blue; some mixtures of anionic dyes could also be effectively separated. To learn the dye-encapsulation and guest-selection mechanism, CAMs with a different core from **3a**−**3d**, i.e., HP(EI-$OH_1C12_{0.15}$) (**4a**), HP(EI-$OH_1C12_{0.30}$) (**4b**), HP(EI-$OH_1C12_{0.60}$) (**4c**), and HP(EI-$OH_1C12_{0.86}$) (**4d**), are synthesized and their property is evaluated; meanwhile, CAMs with a thicker shell, i.e., HP(EI-$OH_{0.15}PS_{0.15}$) (**7a**), HP(EI-$OH_{0.30}PS_{0.30}$) (**7b**), and HP(EI-$OH_{0.60}PS_{0.60}$) (**7c**) (Scheme 1), are also synthesized by alkylation of HPEI with epoxy polystyrene (M_n = 1800), and their dye-encapsulation property is tested.

4a−**4d** are synthesized by complete alkylation of the residual amino protons of **3a**−**3d** in ethanol with propylene oxide, respectively, while **7a**−**7c** are synthesized by alkylation of HPEI with epoxy polystyrene; these CAMs are characterized by ^{1}H NMR measurement. Figure 1 shows the ^{1}H NMR spectra of **3b** and **4b**. From Figure 1A,B it can be found that after the alkylation of **3b** with propylene oxide, new signal at 1.15 ppm (f) appears, which is due to the methyl of ring opened propylene oxide; the signal intensities at 3.8 ppm (OH) and 3.4 ppm (CH) are also enhanced due to signal overlapping of **3b** with the ring-opened propylene oxide. By comparing the signal intensity of (f) and (a) in Figure 1A, it can be derived that the residual amino

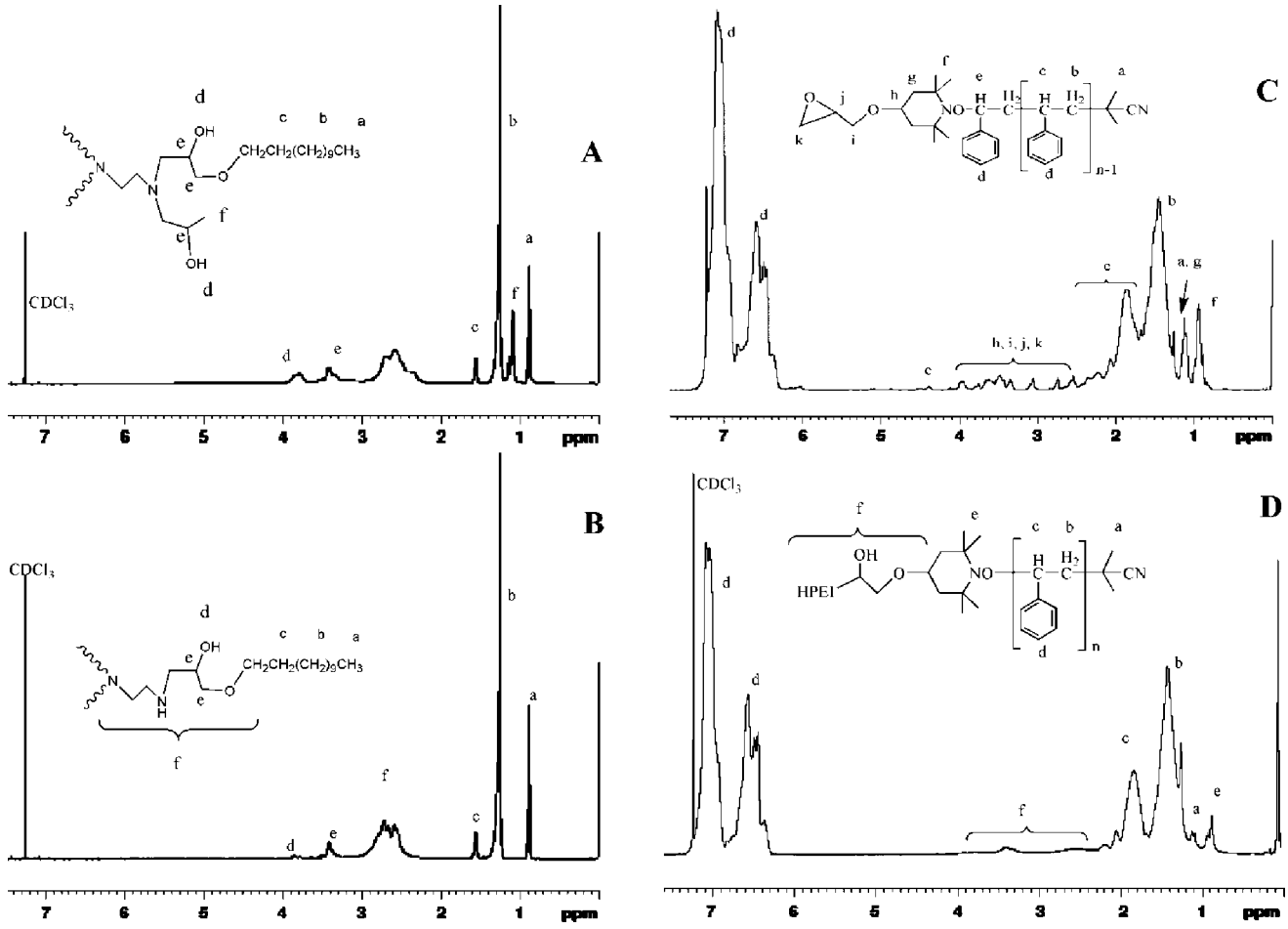

Figure 1. ^{1}H NMR spectra of **3b** (B), **4b** (A), **6** (C), and **7a** (D) in $CDCl_3$.

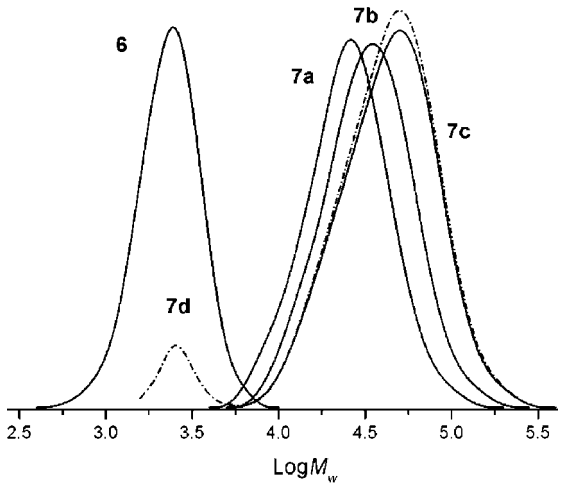

Figure 2. GPC traces of **6**, **7a**−**7c**, and **7d** (the bimodal trace of **7d** suggests it is a mixture).

protons in **3b** have been completely alkylated. Epoxy polystyrene is also synthesized and used to functionalize HPEI; Figure 1C shows the ^{1}H NMR spectrum of the resulting epoxy polystyrene (**6**, $M_n = 1800$), and Figure 1D shows the spectrum of **7a**. The DF of compound **7** can be as high as 60%. GPC measurement shows that within 60% a unimodal GPC chromatograph appears, as shown in Figure 2, but a higher DF is currently not yet available (see **7d** in Figure 2 where bimodal trace indicates a mixed polymers). Table 1 shows the molecular weight of **4a**−**4d** and **7a**−**7c** derived from ^{1}H NMR. The molecular weight (M_n) and molecular weight distribution (M_w/M_n) of **7a**−**7c** are also obtained by GPC measurement, and the data are collected in Table 1. The M_n values derived from ^{1}H NMR spectra are coincident with the calculated values.

Table 1. Molecular Weight and Molecular Weight Distribution of 4a−4d and 7a−7c[a]

CAM	M_n(^{1}H NMR) × 10^{-3}	M_n(GPC) × 10^{-3}	M_w/M_n
4a	31.1		
4b	37.8		
4c	51.0		
4d	60.0		
7a	75.3	28.0	1.51
7b	140.7	47.0	1.53
7c	271.4	67.3	1.55

[a] M_n(^{1}H NMR) is derived from ^{1}H NMR spectra; M_n(GPC) and M_w/M_n are derived from GPC measurement (see experiment).

Among the above CAMs, **4a**−**4d** have almost the same FGs in the core but with different DF; and for the four pairs of **3a/4a**, **3b/4b**, **3c/4c**, and **3d/4d**, each pair has the same DF but different FGs in the core; while for the three pairs of **3a/7a**, **3b/7b**, and **3c/7c**, each pair has the same DF and FG but with different shell thickness.

2. Encapsulation Capacity and Guest Releasing Ability. All the CAMS have a polar core which can interact with hydrophilic guests and have a hydrophobic shell which renders them soluble in a number of apolar organic solvents. It is found that anionic, water-soluble dyes such as MO and CR can be transferred from aqueous phase to organic phase by chloroform solution of the CAMs via a liquid−liquid extraction, while in the absence of the CAM, no coloration of the oil phase is observed, indicating the transferring of dye is due to the CAM.

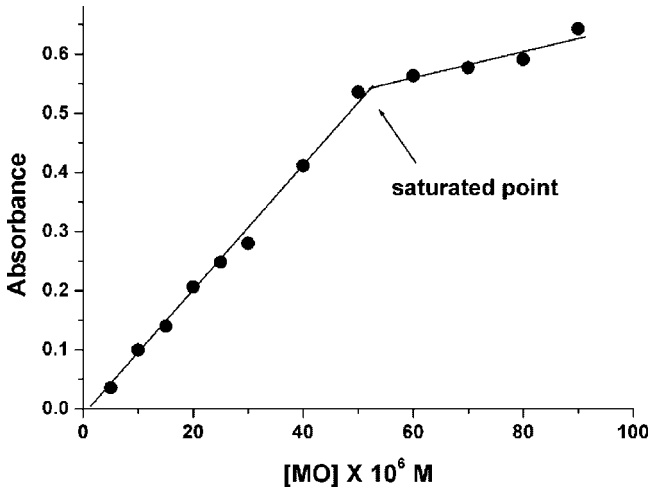

Figure 3. Encapsulation of MO by **4d** in dependence of the concentration of MO. Conditions: [**4b**] = 3.49×10^{-7} M.

Table 2. Comparison of the Encapsulating Ability of 4a−4d with 3a−3d at the Saturated Point[a]

CAM **4** (**3**)	DF (%)	MOs encapsulated (mol/mol)[b]
4a (**3a**)	15	11 (9)
4b (**3b**)	30	85 (75)
4c (**3c**)	60	81 (69)
4d (**3d**)	86	72 (71)

[a] Water/chloroform liquid−liquid extraction of MO, [**4**] = [**3**] = 3.49×10^{-7} M in chloroform. [b] The value in parentheses is the MOs encapsulated by **3a**−**3d**.[5i]

Experimentally, when the CAM−chloroform is exposed to aqueous MO with shaking, the oil layer is colorized while the color in the aqueous layer completely disappears or recedes. To learn the number of dyes one CAM can load, the experiment is repeated by preparing many CAM samples with the same concentration, and each of the samples is exposed to different amount of MOs in water until no more MOs can be transferred to the oil phase. Figure 3 shows a typical two-stage encapsulation character in the case of **4d**: during stage 1, MOs are completely and irreversibly transferred to the oil; during stage 2, extra MOs are transferred to the oil and the encapsulation is reversible; i.e., when washed with fresh water, the extra MOs are released to the water phase. Most probably, during stage 1, MOs complex with the CAM tightly due to a strong host−guest interaction; while during stage 2, guest−guest repulsion becomes important that an excess of guest is present in equilibrium with the complexed guests.[3h] The intercept of stage 1 and stage 2 is regarded as the saturation point, from which the number of MOs encapsulated by one **4d** molecule can be derived. The other CAMs are tested similarly, and the results are collected in Table 2. For convenience of comparison, the encapsulating ability of **3a**−**3d** is also listed in the table. It is found that with the decrease of DF from 86% (**4d**) to 30% (**4b**) the saturated encapsulating ability of the CAMs is slightly enhanced; one possible reason is that a high DF occupies part of the space that could be provided for the guest, as suggested by other researchers.[5g] On the other hand, for CAMs with the same DF but different FGs, the encapsulating ability is dependent on the nature of FGs in the core. For example, all the four pairs of **4**/**3** show that after the primary and secondary amines are transformed into tertiary amines and hydroxyls the encapsulating ability is enhanced at the specified concentration of 3.49×10^{-7} M, indicating the nature of FGs in the core is important for guest encapsulating ability; the core with denser population of tertiary amines and hydroxyls is favorable for stronger guest binding.

It is found that the nature of FGs in the core is crucial to the guest releasing, while DF hardly exerts any influence on the guest releasing property. For example, **3b** and **4b** have the same DF but different FGs in the core; when the MO-saturated chloroform solution of **3b** is subjected to repeated washing with fresh water (each time with equal volume to that of chloroform), the sixth washing time leads to complete decolorization of the oil layer, but in the case of **4b** with the same concentration, up to 86% of the MO molecules keep intact after the sixth washing time, indicating that MOs are favored to reside in the oil phase by the host **4b**. A similar trend is found for the pair of **3c**/**4c**. Thus, it can be concluded that the guest releasing ability is determined by the nature of FGs in the core rather than by the DF. This behavior suggests that the guest encapsulation mainly stems from the physical binding strength between the FGs in the core and the guest; weaker binding strength leads to higher tendency toward guest release, while the shell hardly exerts any influence on guest release. Understanding of this mechanism may be favorable for the design of a host that can confer controlled release of a guest.

3. Aggregation versus Unimolecularity. It is known that if the host exists exclusively as a unimolecular micelle, its encapsulating capacity will be independent of its concentration.[5j] **3d** has been shown with concentration-dependent encapsulating capacity, which is an indication of aggregation.[5i] **3a**−**3c** and **4a**−**4d** most probably also exist as aggregates in chloroform because their encapsulating ability is greatly suppressed with their concentration, as shown in Figure 4. Experimentally, excessive MOs in water are exposed to various amount of CAM in chloroform, and the amount of MOs transferred to the oil is measured by a UV−vis spectrometer. The MOs are in great excess so that a saturated encapsulation can be ensured. It can be found from Figure 4 that in the tested range a nonlinear relationship is shown, which indicates the CAMs exist as aggregate. It can also be found that **3b** and **4b**, both with DF of 30%, show higher encapsulating ability than the others in their respective group, agreeing well with the results in Table 2. It is also noticed that at high concentration the encapsulating capacity of **4a**−**4c** is suppressed to a greater extent than that of **3a**−**3c**, which may be related to their aggregation behavior in solution.

The encapsulation behavior of **4d** is studied in detail. **4d** is prepared in a variety of concentrations in chloroform, and for the sample at each concentration, a saturated encapsulating capacity can be obtained via the method shown in Figure 3. Both CR and MO are tested and the results are collected in Table 3.

It can be found from Table 3 that at 8.56×10^{-7} M one **4d** can averagely encapsulate 23 CR molecules, while at 3.42×10^{-8} M, 216 CR molecules can be encapsulated (~10-fold enhanced), supporting that **4d** exists as aggregate in chloroform. At very low concentration of 1.71×10^{-8} M, encapsulation of CR is no longer observed; even after the chloroform is concentrated by 100-fold, no CR is detected by UV/vis. Most probably, in this case, **4d** no longer exists as aggregate but as free molecule, and the free molecule cannot encapsulate any CR (a similar phenomenon was observed previously by Haag et al.[5d]).

Dynamic light scattering (DLS) shows a critical aggregation concentration (CAC) of 2.23×10^{-8} M for **4d**. At concentration below CAC, only one peak corresponding to a diameter of 19.6 nm is detected by DLS, while right above the CAC, beside the 19.6 nm particles, another peak corresponding to a diameter of 142 nm is also observed. Encapsulation experiment shows that below the CAC no CR can be encapsulated by **4d**, while above the CAC CR can be encapsulated. This is different from MO, where encapsulation occurs both below and above the CAC. These results suggest that MOs can be encapsulated by both

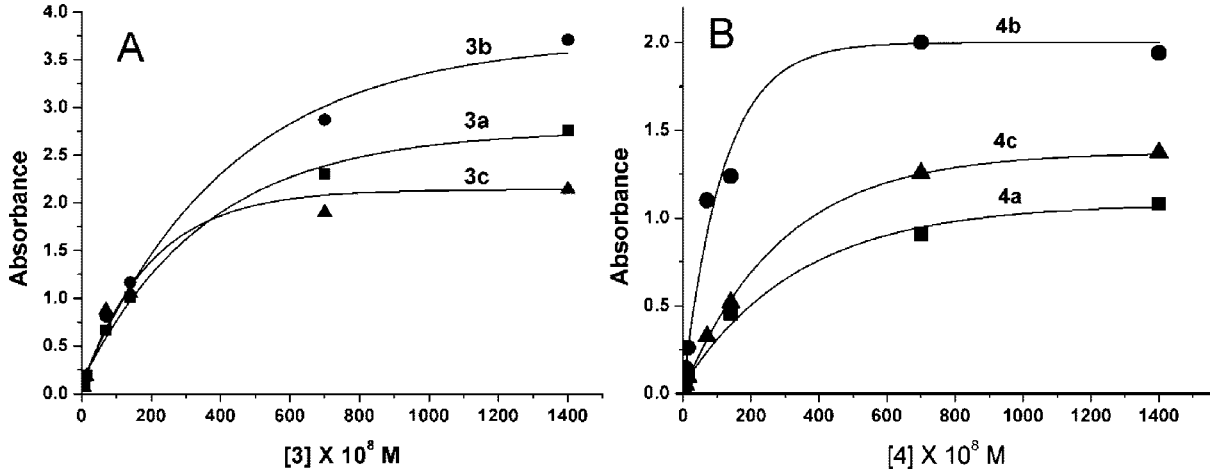

Figure 4. Transport capacity of **3a**−**3c** (A) and **4a**−**4c** (B) in dependence of their concentration. Conditions: liquid−liquid extraction of aqueous MO with CAMs in chloroform, [CAM] = 1.0×10^{-8}−1.4×10^{-5} M, [MO] = 5×10^{-3} M. The curve is the best fit line.

Table 3. Saturated Encapsulating Capacity of 4d in Dependence of its Concentration[a]

4d in $CHCl_3$		MO encapsulated[b]		CR encapsulated[b]	
(M)	(g/L)	(mol/mol)	(g/g)	(mol/mol)	(g/g)
8.56×10^{-7}	0.051	60	0.33	23	0.27
4.28×10^{-7}	0.0257	70	0.43	32	0.37
8.56×10^{-8}	0.0051	128	0.70	118	1.37
3.42×10^{-8}	0.0021	191	1.04	216	2.51
1.71×10^{-8}	0.0011	254	1.38	*c*	*c*

[a] Liquid−liquid extraction of MO (CR) in water by **4d** in chloroform at the saturated point. [b] Molecules of MO (CR) encapsulated by one **4d** molecule (mol/mol) or gram of MOs (CRs) encapsulated per gram of **4d** (g/g). [c] No encapsulation of CR is detected.

Table 4. CAC, Hydrodynamic Diameter (D_h), and Polydispersity Index ($\mu_2/\langle\Gamma\rangle^2$) of 4a−4d Derived from DLS Measurement

sample	CAC × 10^8 (M)	D_h (nm)	$\mu_2/\langle\Gamma\rangle^2$
4a	1.22	120	0.40
4b	1.98	58	0.23
4c	2.11	49	0.15
4d	2.23	142	0.35

the aggregate and the unimolecular micelle, while CR can only be encapsulated by the aggregate. Similarly, CACs, hydrodynamic diameters, and polydispersity index of **4a**−**4c** are also obtained by the DLS measurement, as shown in Table 4. It can be concluded from Table 4 that increase the DF only slightly improves the CAC value of the CAMs.

To further prove that **4d** exists as aggregate, its solution (4.28×10^{-7} M in chloroform) is stained with H_2PtCl_4 before transmission electronic microscopy (TEM) measurement. Experimentally, **4d** in chloroform is stirred with H_2PtCl_4 in excess for a desired time, and the insoluble part is removed; the colloid is diluted and subjected to TEM measurement. Figure 5A shows that after the Pt ions are sequestered by **4d** in chloroform a red shift appears in the UV−vis spectra when compared with that of Pt ions in water. The red shift should stems from the complexation between the Pt ions and the amino group of **4d**. Figure 5B shows the TEM microgram of the colloidal particle, where big globular nanoparticles with diameter between 50 and 150 nm and some very tiny dots are observed. The appearance of the big nanoparticles supports that **4d** exists as aggregate in chloroform. Sample without staining can also be found as aggregate in TEM measurement; Figure 5C shows the case for **4a**. AFM measurement also proves that **4d** exists as aggregate under the current condition, as shown in Figure 5D, where globular and rodlike particles are both observed; the rod may form via the coalescence of globular particles.

It is known that if a CAM exists unimolecularly in solution, its encapsulating ability will be independent of its concentration.[5j] Since a thick shell is generally believed to be favorable for the formation of unimolecular micelle, **7a**−**7c** are synthesized with thick shell, and their encapsulation of MO is tested.

The encapsulation of MO by **7b** is shown in Figure 6, where a three-stage nonlinear encapsulating behavior is observed: during stage 1, MOs in water are completely transferred to the oil layer; during stage 2, an equilibrium exists that only partial MOs are transferred to the oil layer; during stage 3, no MOs are transferred to the oil because a saturation is reached. The encapsulation behavior is very similar to that of **4a**−**4d**. The intercept of stage 1 and stage 2 is regarded as the saturated point, from which the number of MOs encapsulated by one **7b** molecule can be derived; the sample is also tested at other concentrations, and the encapsulating capacity is shown in Table 5. **7a** and **7c** are tested similarly, and the data are also collected in Table 5.

The results in Table 5 show that the encapsulating ability is independent of the concentration of **7a**−**7c** in a very wide range, indicating unimolecular nature of **7a**−**7c**. TEM measurement is carried out similar to **4d**, but no large particles are detected, further supporting that **7a**−**7c** exist as unimolecular micelles. It is interesting that for the sample of **7a** with a DF of only 15% the nature of unimolecular micelle is still found, which is in sharp contrast to **4b**, where a DF of 86% does not ensure the formation of unimolecular micelle. That **7a**, **7b**, and **7c** show an increased encapsulating ability in sequence with DF may be due to their different cores, as discussed previously.

It is noticed that **7a**−**7c** show a much lower apparent encapsulating capacity than **4a**−**4d**; however, the direct comparison of their encapsulating ability is not appropriate and also unfeasible because **7a**−**7c** exist unimolecularly while **4a**−**4d** generally exist as aggregate, though unimolecular micelle of **4a**−**4d** is available at extremely low concentration. Comparison of **3a** with **7a** is interesting: their cores are similar, but the former shows limited solubility in apolar solvent and the encapsulating ability is greatly suppressed at high concentration, while the latter shows good solubility in apolar solvents and the encapsulating ability of each molecule keeps intact with the concentration.

Encapsulation of CR is very different from that of MO. Like MO, CR is an anionic, water-soluble dye but is a rodlike molecule with negative charges on either end (Chart 1). Encapsulation of CR by **4d** is studied in detail. Figure 7 shows the two-stage encapsulation of CR. Strangely, the encapsulation

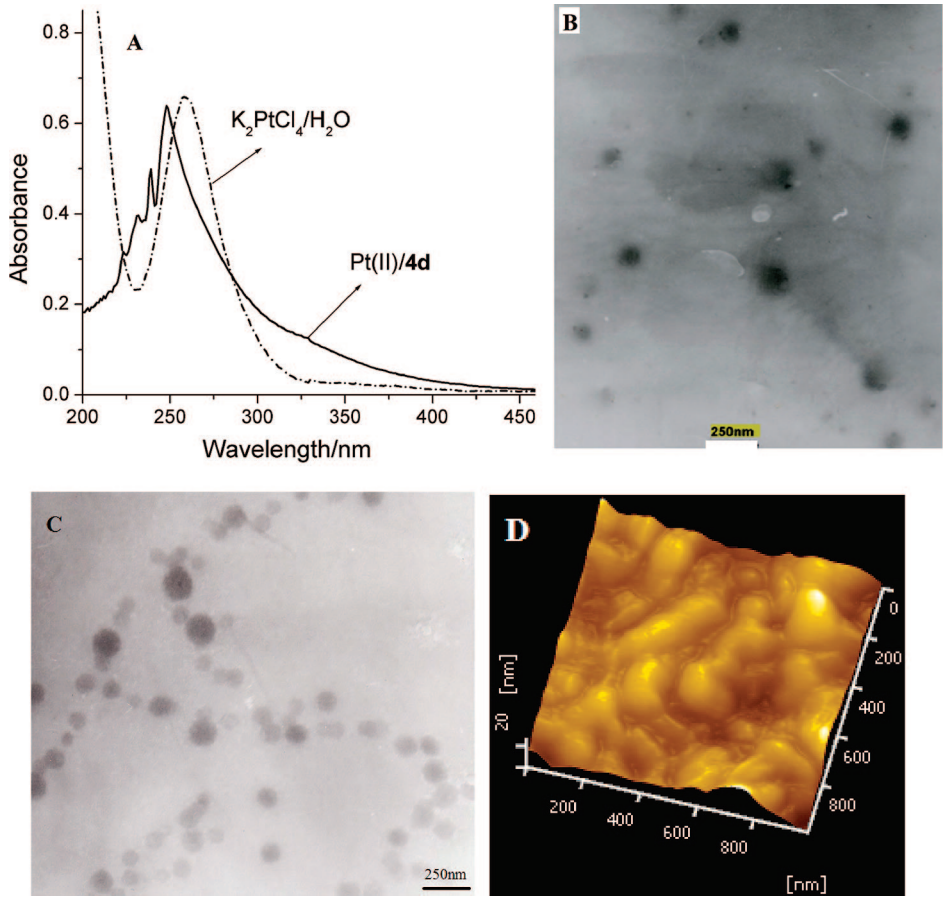

Figure 5. UV−vis spectra of **4d** stained with Pt species in chloroform (A), TEM microgram of Pt/**4d** (B) and of **4a** (C), and AFM microgram of **4d** (D). Conditions: samples were prepared at 4.28×10^{-7} M in chloroform for (A−C) and at 4.28×10^{-6} M for (D), and except for UV−vis measurement, the chloroform is evaporated before measurement.

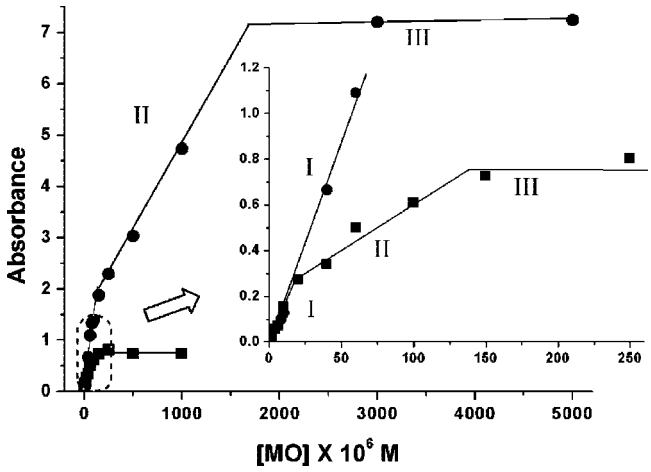

Figure 6. Maximal absorbance of solubilized MOs in dependence of the initial concentration of MO. Conditions: [**7b**] = 8.33×10^{-6} M (●) and 8.33×10^{-7} M (■).

is sensitive to the ratio of CR in the system: before saturation, the encapsulation shows linear increase with the amount of CR, while after a critical (saturated) point the apparent encapsulation suddenly decreases with further addition of CR. One phenomenon helps to understand this behavior: the sudden decreased encapsulation is accompanied by the appearance of precipitate along the oil/water interface. ^{1}H NMR analysis (data not shown) of the precipitate shows the existence of both **4d** and CR. Interestingly, the precipitate gets "dissolved" upon adding more **4d** into the system, indicating the precipitation/colloid transition is dynamic. **3a**−**3d** and **4b**−**4c** are also tested with similar

Table 5. Dependence of Saturated Encapsulation of MO on Concentration of 7a−7c[a]

CAM	concn of CAM (M)	MO encapsulated[b] (mol/mol)
7a	9.6×10^{-6}	8.1
7a	4.8×10^{-6}	8.0
7a	2.4×10^{-6}	8.0
7a	1.92×10^{-6}	7.8
7b	8.33×10^{-6}	12
7b	1.92×10^{-6}	13
7b	8.33×10^{-7}	14
7c	1.92×10^{-6}	16
7c	7.68×10^{-7}	17
7c	1.92×10^{-7}	17
7c	3.42×10^{-8}	18

[a] Liquid−liquid extraction of MO in water by **7** in chloroform. [b] Molecules of MO encapsulated by one CAM molecule.

behavior, but in the case of **3a** and **4a**, much more serious precipitation occurs. We tentatively believe two prerequisites are necessary for the precipitation: (1) existence of CAM aggregate in the system and (2) excessive CRs in the system. Most probably, CRs preferentially dwell in the interior part of the aggregate, and thus before the saturated point, no physical coupling can occur; while in the presence of excessive CRs, extra CRs dwell on the surface of the aggregates and further couple the aggregates physically, which leads to precipitation (much larger aggregates). This may be partly related to the molecular feature of CR, which is rodlike and bears ionic charge on either end, rendering physical coupling of the aggregates possible. In this regards, MO and RB are different in topology from CR and cannot cause similar precipitation.

4. Guest Selection. Since the host−guest binding strength is dependent on the nature of FGs in the core, it is natural that

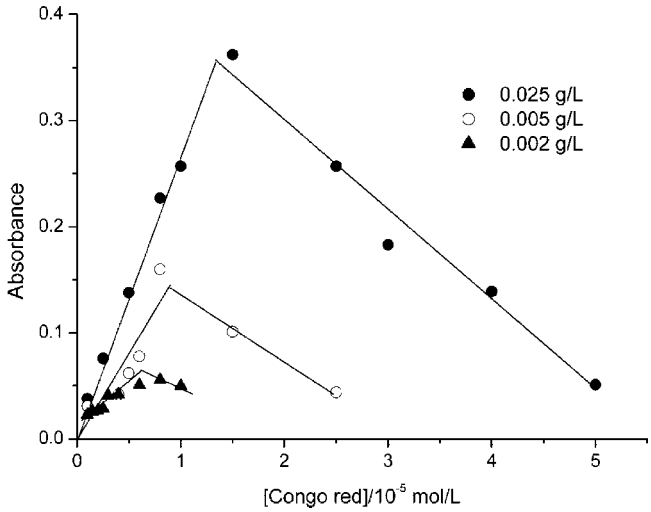

Figure 7. UV−vis absorbance of CR encapsulated by **4d** as a function of $[CR]_0$. Conditions: [**4d**] = 0.025 (●), 0.005 (○), and 0.002 g/L (Δ) or 4.28×10^{-7}, 8.56×10^{-8}, and 3.42×10^{-8} M.

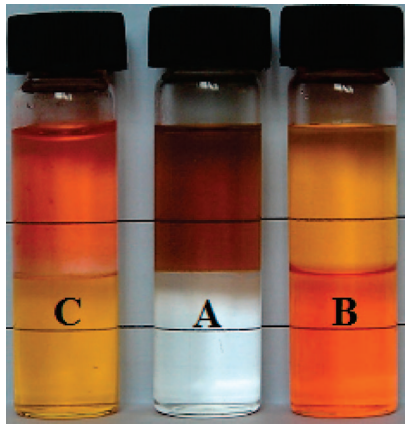

Figure 8. (A) Mixture of MO and CR in biphasic system of water/chloroform. (B) In the presence of a certain amount of **4d**, CR is transferred to the oil phase exclusively. (C) In the presence of certain amount of **7a**, MO is preferentially transferred to the oil phase, where in the oil [MO]/[CR] = 10.5:1.[8] Conditions: $[MO]_0 = [CR]_0 = 4 \times 10^{-5}$ mol/L in water, [**7a**] = 4.45×10^{-6} mol/L, [**4d**] = 5×10^{-7} mol/L in chloroform.

hosts with different cores show different guest affinity. For example, the mixture of MO and CR is hard to be separated via a conventional means but can be conveniently separated by our CAMs. **4d** can exclusively encapsulate CR from the 1:1 mixture of CR/MO, just as **3d** did,[5i] while **7a** selectively encapsulates MO from the same mixture (MO/CR = 10.5/1 in molecule/molecule in **7a**; Figure 8). **3b** and **3c** also show different affinity to CR and MO, but the selectivity is lower than that of **7a** and **4d** because of the mixed FGs in the core of **3b** and **3c**. The selectivity can be understood from the host−guest complement. From the viewpoint of the host, **4d** is more basic in core than **7a** due to the population of tertiary amines; protonation of **4d** will lead to a polar, hydrophilic, and cationic core, while the core of **7a** is less basic, less hydrophilic, and less populated by cations. From the viewpoint of guest, CR bears two anionic charges and is more hydrophilic, while MO bears one anionic charge and meanwhile bears a relatively hydrophobic moiety. Thus, **7a** selects MO while **4d** selects CR. On the other hand, H-bonding interaction should also contribute to the molecular recognition.[1f] It is found that at high pH (pH = 12) the encapsulated MOs are completely expelled by any of the host, while the encapsulated CRs can only be partly expelled by the CAMs, which should be partly attributed to H-bonding interaction between the CR and CAMs. Similar to CR, RB (Chart 1) bears two anionic charges, and the mixture of MO/RB can also be molecularly recognized and separated by our CAMs, though the selectivity is a little lower than that of CR/MO (for example, MO: RB = 88:12 (molecule/molecule) in **7a**, detected by UV−vis spectra). It is worth noticing that the selectivity is independent of the sequence of dye addition, further indicating that the selectivity is not due to topology/size of the dyes but due to the host−guest binding strength.

Conclusion

We have shown that for a CAM derived from hyperbranched polymer the nature of the functional groups in the core is crucial to the guest selection and the guest release, while a thick shell is important in favoring the formation of unimolecular micelle but hardly exerts any influence on guest selection in terms of topology/size. This encapsulation mechanism is important for the CAM design, for example, where controlled release and nature of unimolecular micelle are desired. Moreover, our results indicate that for a host−guest system mainly based on nonspecific ionic interaction highly selective encapsulation is still possible because multisite statistical or cooperative host−guest interaction can amplify the guest binding strength.

Experimental Section

Materials. Hyperbranched polyethylenimnie (HPEI, $M_n = 1 \times 10^4$, $M_w/M_n = 2.5$, degree of branch (DB) = 60%,[5c] Aldrich). 4-Hydroxyl-2,2,6,6-tetramethyl-piperidine-1-oxyl (HTEMPO, kindly presented by Fu-an chemical plant, Wuxi, Jiangsu, China) was purified by recrystallization from hexane. Styrene, propylene oxide, methyl orange (MO), Congo red (CR), and Rose Bengal (RB) were purchased from Sinopharm Chemical Reagent Co. Ltd. (China) with the highest purity available. Styrene was distilled under reduced pressure to remove the inhibitor before use; the other chemicals were used as received except where stated otherwise.

Measurement. UV−vis spectra were recorded on a 760 CRT UV−vis spectrometer. ^{1}H NMR spectra were recorded on Bruker (600 MHz) in $CDCl_3$, with the solvent proton signal or TMS for reference. The number-average molecular weight (M_n) and molecular weight distribution (M_w/M_n) were determined by gel permeation chromatography (GPC) using a Waters 150-C, calibrated with standard poly(styrene); eluent: DMF + 100 mM LiCl; flow rate: 1 mL/min; sample concentration: 10 mg/mL; injection volume 200 μL. Transmission electronic microscopy (TEM) is carried out on a Hitachi H-800, operating with an acceleration voltage of 200 kV. The sample was prepared by dropping a chloroform solution on a carbon-coated copper grid and evaporation of the solvent. Dynamic light scattering (DLS) was recorded on a commercial laser light scattering (LLS) spectrometer (Malvern Autosizer 4700) equipped with a solid-state laser (ILT 5500QSL, output power 100 mW at $\lambda_0 = 532$ nm) as the light source. All the DLS measurements were performed at 25 ± 0.1 °C. Size and polydispersity index ($\mu_2/\langle\Gamma\rangle^2$) were obtained by a CONTIN analysis mode. All the solutions at different concentrations were clarified using a 0.45 μm Millipore filter before the measurements. Atomic force microscopy was recorded on a SPA-300HV via a dynamic force mode, the resolution is 0.2 nm, and the sample was prepared by dropping a chloroform solution (0.02 g/L) on a fresh mica and evaporation of the solvent.

Synthesis. 2-Dodecyloxymethyloxirane (**2**) and **3a**−**3d** were synthesized as previously reported.[5i]

Synthesis of **4** is exemplified by that of **4a**. **3a** (1 g, equivalence of 12.6 mmol of NH) in ethanol (10 mL) was mixed with propylene oxide (1 g, 17.2 mmol) and stirred at room temperature for 3 days. After the volatile was removed on a rotary evaporator, the residual was washed with a small amount of methanol to yield a colorless viscous liquid (1.73 g, 100% yield).

The molecular weight of **4a** is calculated as follows: HPEI can be formulated as $(CH_2CH_2NH)_{242}$, and **3a** (15% of the amino protons are alkylated by 2-dodecyloxymethyloxiane) can be for-

mulated as $[(CH_2CH_2NH)]_{205.7}[CH_2CH_2NCH_2CH(OH)CH_2O-C_{12}H_{25}]_{36.3}$ (FW: 1.92×10^4); after the residual amino protons of **3a** is further alkylated with propylene oxide, the resulting **4a** can be formulated as $[(CH_2CH_2NCH_2CH(OH)CH_3]_{205.7}[CH_2CH_2NCH_2-CH(OH)-CH_2OC_{12}H_{25}]_{36.3}$ (FW: 3.11×10^4).

4-Glycidyloxy-2,2,6,6-tetramethyl-piperidine-1-oxyl (**5**) was synthesized according to the literature.[9]

4-Glycidyloxy-2,2,6,6-tetramethyl-piperidine-1-oxyl-polystyrene (**6**) was synthesized as follows: for [St]/[**5**]/[AIBN] = 30:1:0.6, a mixture of **5** (0.54 g, 2.368 mmol), AIBN (0.233 g, 1.4 mmol), and styrene (7.4 g, 71 mmol) was degassed by bubbling with nitrogen for 15 min, sealed, and heated at 70 °C for 2 h, followed by heating at 125 °C for 37 h. The polymer was recovered by dilution with chloroform and precipitation in ethanol; purification was carried out by repeated dissolving in chloroform and precipitating in ethanol (95%) and finally dried in a vacuum oven at 60 °C for 12 h. 4.53 g (57%) of white powder was obtained. M_n(calcd) = 2000, M_n(GPC) = 1800, M_w/M_n = 1.34.

Synthesis of **7a**−**7c**. Typically, for the preparation of **7a**, a solution of HPEI (0.02 g) and **6** (0.14 g) in DMF (0.5 mL) was stirred at room temperature for 11 days. After most of the DMF was removed under reduced pressure on a rotary evaporator, the polymer was recovered by precipitating in ethanol (95%). The polymer was purified by repeated dissolving in chloroform and precipitating in ethanol and finally dried in a vacuum oven at 60 °C for 12 h. A quantitative yield was obtained.

Dye Encapsulation. *Determination of the Saturated Encapsulation by a CAM*. Generally, a stock solution of a CAM in chloroform (3.49×10^{-7} M) was prepared; aqueous MO at a diversity of concentrations (1×10^{-6}−1×10^{-3} M) was prepared and mixed with equal volume of stock solution under rigorous shaking. After a long standing, each liquid layer became clear, and the oil layer was separated for a UV−vis measurement. For example, **4d** at 3.49×10^{-7} M in $CHCl_3$ was charged evenly in 12 vials (4 mL in each vial), MO (4 mL) at concentrations of 5, 10, 15, 20, 30, 40, 60, 80, 125, 250, 500, and 1000×10^{-6} M in water was added to each of the above vials, and the MOs transferred to the oil were separated for UV−vis measurement. The absorbance data were plotted against the initial concentration of MO to find the deflection point which was regarded as the saturated encapsulation.

Concentration-Dependent Encapsulation. To learn whether a CAM exists as aggregate or as unimolecular micelle, the dependence of encapsulating capacity on concentration of the CAM was measured, where a linear relationship generally means that unimolecular micelle exists exclusively. A stock solution of aqueous MO was prepared; a CAM at a diversity of concentrations was prepared and mixed with equal volume of the stock solution under vigorous shaking ([MO] ≫ [CAM], for example, [MO] = 5×10^{-3} M, while [CAM] = 10^{-5}−10^{-8} M) to ensure a saturated encapsulation). After a phase balance was reached, the oil layer was separated and measured with a UV−vis spectrometer. The absorbance data were plotted against the CAM concentration, where a linear relationship suggests that unimolecular micelle existed exclusively, while a nonlinear one suggests the existence of aggregate.

In case the UV−vis absorbance (A) was less than 0.1 (or larger than 1), the solution was concentrated (diluted) until the A was within 0.1−1, and the absorbance datum was reduced (amplified) to the equivalent concentration.

Stain of the CAM with Pt Ions and Transmission Electronic Microscopy (TEM) Measurement. Typically, H_2PtCl_4 (0.2 g, 0.38 mmol) was stirred with **4d** (1 g) in chloroform (10 mL) for 12 h, the H_2PtCl_4 in excess was removed by filtration, and the yellowish-red chloroform was diluted and subjected to TEM measurement.

Acknowledgment. This work is supported by Shanghai Natural Foundation of China (No. 08ZR1420300). MS Yunfen Cao (Fudan University) is greatly appreciated for the DLS measurement.

References and Notes

(1) (a) Newkome, G. R.; Moorefield, C. N.; Baker, G. R.; Johnson, A. L.; Behera, R. K. *Angew. Chem., Int. Ed.* **1991**, *30*, 1176–1178. (b) Newkome, G. R.; Moorefield, C. N.; Baker, G. R.; Saunders, M. J.; Grossman, S. H. *Angew. Chem., Int. Ed.* **1991**, *30*, 1178–1180. (c) Baars, M. W. P. L.; Meijer, E. W. Dendrimers II. *Top. Curr. Chem.* **2000**, *210*, 131–182. (d) Zimmerman, S. C.; Lawless, L. J. Dendrimers IV. *Top. Curr. Chem.* **2001**, *210*, 951–120. (e) Maciejewski, M. *J. Macromol. Sci., Chem.* **1982**, *17A*, 689. (f) Sunder, A.; Kramer, M.; Hanselmann, R.; Mulhaupt, R.; Frey, H. *Angew. Chem., Int. Ed.* **1999**, *38*, 3552–3555. (g) Duncan, R. *Nat. Rev. Drug Discovery* **2003**, *2*, 347–360. (h) Stiriba, S.-E.; Frey, H.; Haag, R. *Angew. Chem., Int. Ed.* **2002**, *41*, 1329–1334.

(2) (a) Stiriba, S. E.; Kautz, H.; Frey, H. *J. Am. Chem. Soc.* **2002**, *124*, 9698–9699. (b) Pang, X. C.; Wang, G. W.; Jia, Z. F.; Liu, C.; Huang, J. L. *J. Polym. Sci., Part A: Polym. Chem.* **2007**, *45*, 5824–5837. (c) Schmaljohann, D.; Potschke, P.; Hassler, R.; Voit, B. I.; Froehling, P. E.; Mostert, B.; Loontjens, J. A. *Macromolecules* **1999**, *32*, 6333–6339. (d) Wan, D. C.; Pu, H. T. *Mater. Lett.* **2007**, *61*, 3404–3408.

(3) (a) Tomalia, D. A.; Naylor, A.; Goddard, W. A., III. *Angew. Chem., Int. Ed.* **1990**, *29*, 138–175. (b) Frechet, J. M. J. *Science* **1994**, *263*, 1710–1715. (c) Jansen, J. F. G. A.; de Brabander-van den Berg, E. M. M.; Meijer, E. W. *Science* **1994**, *265*, 1226–1229. (d) Jansen, J. F. G. A.; Meijer, E. W. *J. Am. Chem. Soc.* **1995**, *117*, 4417–4418. (e) Tomoyose, Y. T.; Jiang, D.-L.; Jin, R.-H.; Aida, T.; Yamashita, T.; Horie, K.; Yashima, E.; Okamoto, Y. *Macromolecules* **1996**, *29*, 5236–5238. (f) Pollak, K. W.; Leon, J. W.; Frechet, J. M. J.; Maskus, M.; Abruna, H. D. *Chem. Mater.* **1998**, *10*, 30–38. (g) Pistolis, G.; Malliaris, A.; Tsiourvas, D.; Paleos, C. M. *Chem.—Eur. J.* **1999**, *5*, 1440–1444. (h) Baars, M. W. P. L.; Kleppinger, R.; Koch, M. H. J.; Yeu, S. L.; Meijer, E. W. *Angew. Chem., Int. Ed.* **2000**, *39*, 1285–1288.

(4) Gao, C.; Yan, D. Y. *Prog. Polym. Sci.* **2004**, *29*, 183–275.

(5) (a) Garamus, V. M.; Maksimova, T. V.; Kautz, H.; Barriau, E.; Frey, H.; Schlotterbeck, U.; Mecking, S.; Richtering, W. *Macromolecules* **2004**, *37*, 8394–8399. (b) Chen, Y.; Shen, Z.; Pastor-Perez, L.; Frey, H.; Stiriba, S. E. *Macromolecules* **2005**, *38*, 227–229. (c) Liu, H. J.; Chen, Y.; Zhu, D. D.; Shen, Z.; Stiriba, S. E. *React. Funct. Polym.* **2007**, *67*, 383–395. (d) Kramer, M.; Kopagzynska, M.; Krause, S.; Haag, R. *J. Polym. Sci., Part A: Polym. Chem.* **2007**, *45*, 2287–2303. (e) Liu, C. H.; Gao, C.; Yan, D. Y. *Macromolecules* **2005**, *39*, 8102–8111. (f) Kitajyo, Y.; Nawa, Y.; Tamaki, M.; Tani, H.; Takahashi, K.; Kaga, H.; Satoh, T.; Kakuchi, T. *Polymer* **2007**, *48*, 4683–4690. (g) Kitajyo, Y.; Imai, T.; Sakai, Y.; Tamaki, M.; Tani, H.; Takahashi, K.; Narumi, A.; Kaga, H.; Kaneko, N.; Satoh, T.; Kakuchi, T. *Polymer* **2007**, *48*, 1237–1244. (h) Satoh, T.; Tamaki, M.; Kitajyo, Y.; Maeda, T.; Ishihara, H.; Imai, T.; Kaga, H.; Kakuchi, T. *J. Polym. Sci., Part A: Polym. Chem.* **2006**, *44*, 406–413. (i) Wan, D. C.; Pu, H. T.; Cai, X. Y. *Macromolecules* **2008**, *41*, 7787–7789. (j) Hawker, C. J.; Chu, F. K. *Macromolecules* **1996**, *29*, 4370–4380.

(6) (a) Radowski, M. R.; Shukla, A.; von Berlepsch, H.; Bottcher, C.; Pickaert, G.; Rehage, H.; Haag, R. *Angew. Chem., Int. Ed.* **2007**, *46*, 1265–1269. (b) Xu, S. J.; Luo, Y.; Haag, R. *Macromol. Rapid Commun.* **2008**, *29*, 171–174.

(7) Nomenclature: for example, HP(EI-OH_xC12_y) means a fraction (x) of the amino protons are derived into hydroxyls and a fraction (y) of amino groups are alkylated by 2-dodecyloxymethyloxirane.

(8) Quantitative analysis of the ratio of encapsulated MO and CR is impossible because of the featureless UV/vis and signal overlapping of ^{1}H NMR spectra, but a rough value can be obtained from UV−vis spectra because the λ_{max} is sensitive to the ratio of CR/MO. Experimentally, when aqueous CR is shaken with the MO-saturated **7a**/chloroform, the dye exchange will lead to a shift of the aqueous λ_{max}. To learn the λ_{max}−(CR/MO) relationship, a simulation experiment is carried out by titration-like addition of aqueous MO to the aqueous CR (the concentration of CR is the same) until the same shift of λ_{max} is reached. It is known the λ_{max} is slightly sensitive to the concentration and medium, so the simulation is carried out under very similar conditions that a relatively countable result can be obtained.

(9) Jia, Z. F.; Fu, Q.; Huang, J. L. *J. Polym. Chem., Part A: Polym. Chem.* **2006**, *44*, 3836–3842.

MA8026707